DOI: https://doi.org/10.15407/pmach2025.02.027

UDC 534.1

LINEAR VIBRATIONS ANALYSIS OF A COMPOSITE SANDWICH CONICAL SHELL MANUFACTURED BY ADDITIVE TECHNOLOGIES

[1] Kostiantyn V. Avramov
kvavramov@gmail.com,
ORCID: 0000-0002-8740-693X

[1] Borys V. Uspenskyi
Uspensky.kubes@gmail.com,
ORCID: 0000-0001-6360-7430

[2] Borys H. Liubarskyi
ORCID: 0000-0002-2985-7345

[2] Oleksii A. Smetskykh
ORCID: 0009-0005-0238-9712

[1] Anatolii Pidhornyi Institute of Power Machines and Systems of NAS of Ukraine,
2/10, Komunalnykiv str., Kharkiv, 61046, Ukraine

[2] National Technical University "Kharkiv Polytechnic Institute",
2, Kyrpychova str., Kharkiv, 61002, Ukraine

The sandwich conical shell with elastic honeycomb structure, which is studied in this paper, is manufactured by additive technologies and has three layers. The honeycomb structure is made of ULTEM material, and the upper and lower face layers of the structures are made of carbon fiber. Each layer of the structures is an orthotropic material and satisfies Hooke's law. Thanks to the homogenization procedure using the finite element method, we will obtain an equivalent orthotropic medium instead of the honeycomb structure. The elastic properties of this medium satisfy Hooke's law. The modified high-order shear theory is used to model the deformation of the structures. The deformations of each layer of the structures are described by five variables, which include three projections of the displacements of the median surface and two angles of rotation of the normal to the median surface. To calculate the displacements of the layers, boundary conditions for stresses and boundary conditions that describe the continuity of displacements at the layers' boundaries are used. The vibrations of a three-layer sandwich shell are expanded into basis functions that satisfy the kinematic boundary conditions. The Rayleigh-Ritz method is used to study the vibrations. The vibration parameters of structures are calculated from the eigenvalue problem. To verify the obtained results, the natural frequencies are compared with the data of finite element modeling. As follows from the calculations, the natural frequencies obtained by the Rayleigh-Ritz method and the finite element method are close. The spectrum of natural frequencies is very dense. The minimum natural frequency of vibrations is observed when the number of waves in the circular direction is equal to one.

***Keywords**: sandwich conical shell, honeycomb structure, linear vibrations.*

Introduction

Thin-walled honeycomb sandwich structures are used in aircrafts, rocket launchers, etc. They have high strength and rigidity at low weight. Much effort has been put into studying the mechanical properties of sandwich structures. Nonlinear vibrations of a composite shell of double curvature with an elastic middle layer and a magnetorheological layer are studied in [1]. Nonlinear vibrations of a composite double curvature sandwich shell with a piezoelectric layer are studied in [2]. To obtain a mathematical model, the high-order shear theory and the geometrically nonlinear von Kármán deformation theory are used. The nonlinear dynamic behavior of a sandwich shell of double curvature with an auxetic honeycomb structure with a negative Poisson's ratio is studied in [3], and the geometrically nonlinear vibrations of a closed cylindrical sandwich shell are studied in [4]. Nonlinear vibrations of a cylindrical panel on an elastic foundation under impact loading are studied in [5]. The upper and lower layers are made of a nanocomposite, and the sandwich panel is made of an auxetic honeycomb structure and the face layers are made of a nanocomposite.

Nonlinear equations of motion of a double-curvature sandwich shell with honeycomb structures under transverse loading are derived using Hamilton's variational principle and the Reddy's third-order shear deformation plate theory [6]. Nonlinear vibrations of a multilayer composite shell in a hydrothermal environment are considered in [7]. A nonlinear finite element approach is used to analyze geometrically nonlinear vibrations of sandwich plates with a functionally gradient honeycomb structure [8]. Geometrically nonlinear forced vibrations of a rectangular sandwich panel with a honeycomb structure are described by a system of nonlinear ordinary differential equations, which are solved by the homotopy method [9]. The homogenization method is used to analyze geometrically nonlinear vibrations of sandwich panels in [10].

In this paper, linear vibrations of a sandwich conical shell with a honeycomb structure manufactured using additive technologies, as well as with upper and lower layers of carbon fiber, are studied. The stressed state of each layer is described by five variables, which include three projections of displacements of the median surfaces of each layer and two angles of rotation of the normal to the median surfaces of each layer. To obtain the equations of vibration of structures, the theory of high-order shear and the condition of continuity of displacements between layers are used. Using the Rayleigh-Ritz method, the analysis of linear vibrations is reduced to an eigenvalue problem, from which the parameters of linear vibrations of multilayer structures are obtained. The properties of linear vibrations are studied.

Problem formulation and basic equations

The three-layer sandwich conical shell is shown in Fig. 1. The middle layer of this shell is a honeycomb structure, which is manufactured using additive technology from ULTEM 9085 material. The upper and lower layers are made of carbon fiber. The material of all three layers is orthotropic and satisfies Hooke's law.

Three curvilinear coordinate systems are used to describe the deformation of each layer: (s_t, θ, z_t), (s_c, θ, z_c), (s_b, θ, z_b), where θ is the circular coordinate; z_t, z_c, z_b are transverse coordinates; s_t, s_c, s_b are longitudinal coordinates.

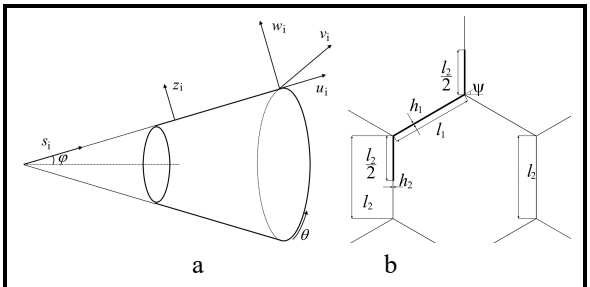

Fig. 1. Sandwich conical shell (a) and honeycomb structure cell (b)

By applying the homogenization procedure [11], we obtain an equivalent orthotropic medium instead of the honeycomb structure. Hooke's law for this medium has the following form:

$$\begin{bmatrix} \sigma_{ss}^{(c)} \\ \sigma_{\theta\theta}^{(c)} \\ \sigma_{zz}^{(c)} \\ \sigma_{\theta z}^{(c)} \\ \sigma_{sz}^{(c)} \\ \sigma_{s\theta}^{(c)} \end{bmatrix} = \begin{bmatrix} C_{11} & C_{12} & C_{13} & 0 & 0 & 0 \\ C_{21} & C_{22} & C_{23} & 0 & 0 & 0 \\ C_{31} & C_{32} & C_{33} & 0 & 0 & 0 \\ 0 & 0 & 0 & C_{44} & 0 & 0 \\ 0 & 0 & 0 & 0 & C_{55} & 0 \\ 0 & 0 & 0 & 0 & 0 & C_{66} \end{bmatrix} \cdot \begin{bmatrix} \varepsilon_{ss}^{(c)} \\ \varepsilon_{\theta\theta}^{(c)} \\ \varepsilon_{zz}^{(c)} \\ 2\varepsilon_{\theta z}^{(c)} \\ 2\varepsilon_{sz}^{(c)} \\ 2\varepsilon_{s\theta}^{(c)} \end{bmatrix}, \tag{1}$$

where $\sigma_{ss}^{(c)}$, $\sigma_{\theta\theta}^{(c)}$, $\sigma_{zz}^{(c)}$, $\sigma_{\theta z}^{(c)}$, $\sigma_{sz}^{(c)}$, $\sigma_{s\theta}^{(c)}$, $\varepsilon_{ss}^{(c)}$, $\varepsilon_{\theta\theta}^{(c)}$, $\varepsilon_{zz}^{(c)}$, $\varepsilon_{\theta z}^{(c)}$, $\varepsilon_{sz}^{(c)}$, $\varepsilon_{s\theta}^{(c)}$ are elements of stress and strain tensors. The upper and lower face layers are made of carbon fiber composite. Hooke's law in this case takes the following form:

$$\begin{bmatrix} \sigma_{ss}^{(j)} \\ \sigma_{\theta\theta}^{(j)} \end{bmatrix} = \begin{bmatrix} \overline{C}_{11} & \overline{C}_{21} \\ \overline{C}_{12} & \overline{C}_{22} \end{bmatrix} \cdot \begin{bmatrix} \varepsilon_{ss}^{(j)} \\ \varepsilon_{\theta\theta}^{(j)} \end{bmatrix};$$

$$\sigma_{s\theta}^{(j)} = 2\overline{C}_{33}\varepsilon_{s\theta}^{(j)}; \quad \sigma_{sz}^{(j)} = 2\overline{C}_{44}\varepsilon_{sz}^{(j)}; \quad \sigma_{\theta z}^{(j)} = 2\overline{C}_{55}\varepsilon_{\theta z}^{(j)}; \; j=b, t.$$

Displacements of the upper and lower layers $u_1^{(i)}$, $u_2^{(i)}$, $u_3^{(i)}$ ($i=t, b$) expand like this:

$$u_1^{(c)} = u^{(i)} + z_i\varphi_1^{(i)} + z_i^2\psi_1^{(i)};$$

$$u_2^{(c)} = \left(1 + \frac{z_i}{\left(s_i^{(1)} + \xi\right)\tan\varphi}\right)v^{(i)} + z_i\varphi_2^{(i)} + z_i^2\psi_2^{(i)}; \quad u_3^{(c)} = w^{(i)}; \quad i=t, b, \tag{2}$$

where $u^{(i)}$, $v^{(i)}$, $w^{(i)}$ are projections of displacements of points of the median surface of layers; $\varphi_1^{(i)}$, $\varphi_2^{(i)}$ are angles of rotation of the normal to the median surface; $\psi_1^{(i)}$, $\psi_2^{(i)}$ are unknown functions that are being calculated. Projections of the displacements of the homogenized layer $u_1^{(c)}$, $u_2^{(c)}$, $u_3^{(c)}$ have the form

$$u_1^{(c)} = u^{(c)} + z_c\varphi_1^{(c)} + z_c^2\psi_1^{(c)} + z_c^3\gamma_1^{(c)};$$

$$u_2^{(c)} = \left(1 + \frac{z_i}{\left(s_{ic}^{(1)} + \xi\right)\tan\varphi}\right)v^{(c)} + z_c\varphi_2^{(c)} + z_c^2\psi_2^{(c)} + z_c^3\gamma_2^{(c)};$$

$$u_3^{(c)} = w^{(c)} + z_c w_1^{(c)} + z_c^2 w_2^{(c)}, \tag{3}$$

where $u^{(c)}$, $v^{(c)}$, $w^{(c)}$ are projections of displacements of the median surface of the homogenized layer; $\varphi_1^{(c)}$, $\varphi_2^{(c)}$ are angles of rotation of the normal to the median surface; $\psi_1^{(c)}$, $\psi_2^{(c)}$, $\gamma_1^{(c)}$, $\gamma_2^{(c)}$, $w_1^{(c)}$, $w_2^{(c)}$ are unknown functions that are being calculated.

Boundary conditions for the stresses of the upper and lower layers are used in the form

$$\sigma_{sz}\big|_{z_t=0.5h_t} = \sigma_{\theta z}\big|_{z_t=0.5h_t} = 0; \quad \sigma_{sz}\big|_{z_b=-0.5h_b} = \sigma_{\theta z}\big|_{z_b=-0.5h_b} = 0, \tag{4}$$

where h_t, h_b are thicknesses of the lower and upper layers. The continuity of displacements at the layer boundaries is described by the following boundary conditions:

$$u_t(z_t = -0.5h_t) = u_c(z_c = 0.5h_c); \quad v_t(z_t = -0.5h_t) = v_c(z_c = 0.5h_c);$$

$$w_t(z_t = -0.5h_t) = w_c(z_c = 0.5h_c); \quad u_b(z_b = 0.5h_b) = u_c(z_c = -0.5h_c);$$

$$v_b(z_b = 0.5h_b) = v_c(z_c = -0.5h_c); \quad w_b(z_b = 0.5h_b) = w_c(z_c = -0.5h_c), \tag{5}$$

where h_c is the thickness of the homogenized layer.

The parameters of the expansions (2, 3) are found from the boundary conditions (4, 5) as follows:

$$\psi_1^{(c)} = -\frac{1}{h_t}\left(\varphi_1^{(t)} + \frac{\partial w^{(t)}}{\partial \xi}\right); \quad \psi_2^{(c)} = -\frac{1}{h_t f_1(\xi)}\left(\varphi_2^{(t)} + \frac{1}{\left(s_t^{(1)} + \xi\right)\sin\varphi}\frac{\partial w^{(t)}}{\partial \theta}\right);$$

$$\psi_1^{(b)} = -\frac{1}{h_b}\left(\varphi_1^{(b)} + \frac{\partial w^{(b)}}{\partial \xi}\right); \quad \psi_2^{(b)} = -\frac{1}{h_b f_2(\xi)}\left(\varphi_2^{(b)} + \frac{1}{\left(s_b^{(1)} + \xi\right)\sin\varphi}\frac{\partial w^{(b)}}{\partial \theta}\right);$$

$$\psi_1^{(c)} = \frac{2}{h_c^2}\left\{u^{(t)} + u^{(b)} - 2u^{(c)} + 0.75h_b\varphi_1^{(b)} - 0.75h_t\varphi_1^{(t)} + \frac{h_b}{4}\frac{\partial w^{(b)}}{\partial \xi} - \frac{h_t}{4}\frac{\partial w^{(t)}}{\partial \xi}\right\};$$

$$\gamma_1^{(c)} = \frac{4}{h_c^3}\left\{u^{(t)} - u^{(b)} - h_c\varphi_1^{(c)} - 0.75h_b\varphi_1^{(b)} - 0.75h_t\varphi_1^{(t)} - \frac{h_b}{4}\frac{\partial w^{(b)}}{\partial \xi} - \frac{h_t}{4}\frac{\partial w^{(t)}}{\partial \xi}\right\};$$

$$\psi_2^{(c)} = \frac{2}{h_c^2}\left\{f_3(\xi)v^{(t)} + f_4(\xi)v^{(b)} - \frac{h_t}{2}\left[1 + \frac{1}{2f_1(\xi)}\right]\varphi_2^{(t)} + \frac{h_b}{2}\left[1 + \frac{1}{2f_2(\xi)}\right]\varphi_2^{(b)} - \right.$$

$$\left. - \frac{h_t}{4f_1(\xi)\left(s_t^{(1)} + \xi\right)\sin\varphi}\frac{\partial w^{(t)}}{\partial \theta} + \frac{h_b}{4f_2(\xi)\left(s_b^{(1)} + \xi\right)\sin\varphi}\frac{\partial w^{(b)}}{\partial \theta} - 2v^{(c)}\right\};$$

$$\gamma_2^{(c)} = \frac{4}{h_c^3}\left\{f_3(\xi)v^{(t)} - f_4(\xi)v^{(b)} - \frac{h_t}{2}\left[1 + \frac{1}{2f_1(\xi)}\right]\varphi_2^{(t)} - \frac{h_b}{2}\left[1 + \frac{1}{2f_2(\xi)}\right]\varphi_2^{(b)} - \right.$$

$$\left. - \frac{h_t}{4f_1(\xi)\left(s_t^{(1)} + \xi\right)\sin\varphi}\frac{\partial w^{(t)}}{\partial \theta} - \frac{h_b}{4f_2(\xi)\left(s_b^{(1)} + \xi\right)\sin\varphi}\frac{\partial w^{(b)}}{\partial \theta} - \frac{h_c}{\left(s_c^{(1)} + \xi\right)\tan\varphi}v^{(c)} - h_c\varphi_2^{(c)}\right\};$$

$$w_2^{(c)} = \frac{2}{h_c^2}\left(w^{(t)} + w^{(b)} - 2w^{(c)}\right); \; w_1^{(c)} = \frac{1}{h_c}\left(w^{(t)} - w^{(b)}\right),$$

where $f_1(\xi) = 1 + \dfrac{h_t}{4(s_t^{(1)} + \xi)\tan\varphi}$; $f_2(\xi) = 1 - \dfrac{h_b}{4(s_b^{(1)} + \xi)\tan\varphi}$; $f_3(s_t) = 1 - \dfrac{h_t}{2(s_t^{(1)} + \xi)\tan\varphi}$;

$f_2(s_b) = 1 + \dfrac{h_b}{2(s_b^{(1)} + \xi)\tan\varphi}$.

The deformations and displacements satisfy the following equations [12]:

$$\varepsilon_{ss}^{(i)}=\frac{1}{1+\dfrac{z_i}{R_s^{(i)}}}\left(\frac{1}{A_s^{(i)}}\frac{\partial u_1^{(i)}}{\partial\alpha_1}+\frac{1}{A_s^{(i)}A_\theta^{(i)}}\frac{\partial A_s^{(i)}}{\partial\alpha_2}u_2^{(i)}+\frac{u_3^{(i)}}{R_s^{(i)}}\right);$$

$$\varepsilon_{\theta\theta}^{(i)}=\frac{1}{1+\dfrac{z_i}{R_\theta^{(i)}}}\left(\frac{1}{A_\theta^{(i)}}\frac{\partial u_2^{(i)}}{\partial\alpha_2}+\frac{1}{A_s^{(i)}A_\theta^{(i)}}\frac{\partial A_\theta^{(i)}}{\partial\alpha_1}u_1^{(i)}+\frac{u_3^{(i)}}{R_\theta^{(i)}}\right);$$

$$\varepsilon_{s\theta}^{(i)}=\frac{1}{1+\dfrac{z_i}{R_s^{(i)}}}\left(\frac{1}{A_s^{(i)}}\frac{\partial u_2^{(i)}}{\partial\alpha_1}-\frac{1}{A_s^{(i)}A_\theta^{(i)}}\frac{\partial A_s^{(i)}}{\partial\alpha_2}u_1^{(i)}\right)+\frac{1}{1+\dfrac{z_i}{R_\theta^{(i)}}}\left(\frac{1}{A_\theta^{(i)}}\frac{\partial u_1^{(i)}}{\partial\alpha_2}-\frac{1}{A_s^{(i)}A_\theta^{(i)}}\frac{\partial A_\theta^{(i)}}{\partial\alpha_1}u_2^{(i)}\right);$$

$$\varepsilon_{sz}^{(i)}=\frac{\partial u_1^{(i)}}{\partial z_i}+\frac{1}{1+\dfrac{z_i}{R_s^{(i)}}}\left[\frac{1}{A_s^{(i)}}\frac{\partial u_3^{(i)}}{\partial\alpha_1}-\frac{u_1^{(i)}}{R_s^{(i)}}\right];\quad \varepsilon_{\theta z}^{(i)}=\frac{\partial u_2^{(i)}}{\partial z_i}+\frac{1}{1+\dfrac{z_i}{R_\theta^{(i)}}}\left[\frac{1}{A_\theta^{(i)}}\frac{\partial u_3^{(i)}}{\partial\alpha_2}-\frac{u_2^{(i)}}{R_\theta^{(i)}}\right];\tag{6}$$

$$i=t,\ c,\ b;\quad \alpha_1\equiv s_i;\quad \alpha_2\equiv\theta.$$

Equations (2, 3) are introduced into (6). As a result, the following asymptotic expansions for the components of the strain tensor are obtained:

$$\varepsilon_{ss}^{(i)}=\varepsilon_{s,0}^{(i)}+z_ik_{s,0}^{(i)}+z_i^2k_{s,1}^{(i)}+z_i^3k_{s,2}^{(i)};$$

$$\varepsilon_{\theta\theta}^{(i)}=\varepsilon_{\theta,0}^{(i)}+z_ik_{\theta,0}^{(i)}+z_i^2k_{\theta,1}^{(i)}+z_i^3k_{\theta,2}^{(i)};$$

$$\varepsilon_{s\theta}^{(i)}=\varepsilon_{s\theta,0}^{(i)}+z_ik_{s\theta,0}^{(i)}+z_i^2k_{s\theta,1}^{(i)}+z_i^3k_{s\theta,2}^{(i)};$$

$$\varepsilon_{sz}^{(i)}=\varepsilon_{sz,0}^{(i)}+z_ik_{sz,0}^{(i)}+z_i^2k_{sz,1}^{(i)}+z_i^3k_{sz,2}^{(i)};$$

$$\varepsilon_{\theta z}^{(i)}=\varepsilon_{\theta z,0}^{(i)}+z_ik_{\theta z,0}^{(i)}+z_i^2k_{\theta z,1}^{(i)}+z_i^3k_{\theta z,2}^{(i)};\ \ i=t,\ c,\ b;$$

$$\varepsilon_{zz}^{(c)}=\varepsilon_{z,0}^{(c)}+z_ck_{z,0}^{(c)},$$

where the values of the components of the expansions are not given for brevity

The potential energy of the upper and lower layers has the following form:

$$U_i=0.5\int_{\overline{V}_i}\left(\sigma_{ss}^{(i)}\varepsilon_{ss}^{(i)}+\sigma_{\theta\theta}^{(i)}\varepsilon_{\theta\theta}^{(i)}+\sigma_{\theta z}^{(i)}\varepsilon_{\theta z}^{(i)}+\sigma_{sz}^{(i)}\varepsilon_{sz}^{(i)}+\sigma_{s\theta}^{(i)}\varepsilon_{s\theta}^{(i)}\right)\left(1+\frac{z_i}{(s_i^{(1)}+\xi)\tan\varphi}\right)\left(s_i^{(1)}+\xi\right)\sin\varphi\cdot d\xi\cdot d\theta\cdot dz_i=$$

$$=0.5\int_{\overline{V}_i}\left(\overline{C}_{11}\varepsilon_{ss}^{(i)2}+\overline{C}_{22}\varepsilon_{\theta\theta}^{(i)2}+2\overline{C}_{12}\varepsilon_{ss}^{(i)}\varepsilon_{\theta\theta}^{(i)}+2\overline{C}_{55}\varepsilon_{\theta z}^{(i)2}+2\overline{C}_{44}\varepsilon_{sz}^{(i)2}+2\overline{C}_{33}\varepsilon_{s\theta}^{(i)2}\right)\left(1+\frac{z_i}{(s_i^{(1)}+\xi)\tan\varphi}\right)\left(s_i^{(1)}+\xi\right)\sin\varphi\cdot d\xi\cdot d\theta\cdot dz_i;$$

$$i=t,\ b,\tag{7}$$

where $\overline{V}_i$ is the volume of the layer i; A_i is the plane of the median surface of the layer.

The potential energy of the homogenized layer has the following form:

$$U_c=0.5\int_{\overline{V}_c}\left(\sigma_{ss}^{(c)}\varepsilon_{ss}^{(c)}+\sigma_{\theta\theta}^{(c)}\varepsilon_{\theta\theta}^{(c)}+\sigma_{zz}^{(c)}\varepsilon_{zz}^{(c)}+\sigma_{\theta z}^{(c)}\varepsilon_{\theta z}^{(c)}+\sigma_{sz}^{(c)}\varepsilon_{sz}^{(c)}+\sigma_{s\theta}^{(c)}\varepsilon_{s\theta}^{(c)}\right)\left(1+\frac{z_c}{(s_c^{(1)}+\xi)\tan\varphi}\right)\left(s_c^{(1)}+\xi\right)\sin\varphi\cdot d\xi\cdot d\theta\cdot dz_c=$$

$$=0.5\int_{\overline{V}_i}\left(C_{11}\varepsilon_{ss}^{(c)2}+C_{22}\varepsilon_{\theta\theta}^{(c)2}+C_{33}\varepsilon_{zz}^{(c)2}+2C_{12}\varepsilon_{ss}^{(i)}\varepsilon_{\theta\theta}^{(i)}+2C_{13}\varepsilon_{ss}^{(c)}\varepsilon_{zz}^{(c)}+2C_{23}\varepsilon_{\theta\theta}^{(c)}\varepsilon_{zz}^{(c)}+2C_{44}\varepsilon_{\theta z}^{(i)2}+2C_{55}\varepsilon_{sz}^{(i)2}+2C_{66}\varepsilon_{s\theta}^{(i)2}\right)\times$$

$$\times\left(1+\frac{z_c}{(s_c^{(1)}+\xi)\tan\varphi}\right)\left(s_c^{(1)}+\xi\right)\sin\varphi\cdot d\xi\cdot d\theta\cdot dz_c.\tag{8}$$

The kinetic energy of the shell layers can be given as

$$T_i = 0.5\int_0^{2\pi}\int_{s_i^{(1)}}^{s_i^{(2)}}\int_{-0.5h_i}^{0.5h_i}\rho_i\left(\dot{u}_1^{(i)2}+\dot{u}_2^{(i)2}+\dot{u}_3^{(i)2}\right)\left(1+\frac{z_i}{(s_i^{(1)}+\xi)\tan\varphi}\right)\left(s_i^{(1)}+\xi\right)\sin\varphi\cdot d\theta\cdot d\xi\cdot dz_i\,;\ i=t,\,c,\,b, \tag{9}$$

where ρ_i is the density of layer materials; $\dot{u}_1^{(i)}=\dfrac{\partial u_1^{(i)}}{\partial t}$.

Linear vibrations analysis

The Rayleigh-Ritz method is used to analyze linear vibrations of a thin-walled structure. In this case, the force boundary conditions of the structures are not taken into account. However, the kinematic boundary conditions are necessarily taken into account. A conical shell clamped at both ends has the following boundary conditions:

$$w^{(i)}\Big|_{s_i=s_i^{(1)}}=v^{(i)}\Big|_{s_i=s_i^{(1)}}=u^{(i)}\Big|_{s_i=s_i^{(1)}}=\varphi_1^{(i)}\Big|_{s_i=s_i^{(1)}}=\varphi_2^{(i)}\Big|_{s_i=s_i^{(1)}}=0\,;$$

$$w^{(i)}\Big|_{s_i=s_i^{(2)}}=v^{(i)}\Big|_{s_i=s_i^{(2)}}=u^{(i)}\Big|_{s_i=s_i^{(2)}}=\varphi_1^{(i)}\Big|_{s_i=s_i^{(2)}}=\varphi_2^{(i)}\Big|_{s_i=s_i^{(2)}}=0\,;\ i=t,\,c,\,b. \tag{10}$$

The vibrations of thin-walled structure have the following form:

$$\begin{bmatrix}u^{(i)}\\ v^{(i)}\\ w^{(i)}\\ \varphi_1^{(i)}\\ \varphi_2^{(i)}\end{bmatrix}=\begin{bmatrix}U_i(\xi)\cos(n\theta)\\ V_i(\xi)\sin(n\theta)\\ W_i(\xi)\cos(n\theta)\\ X_i(\xi)\cos(n\theta)\\ Y_i(\xi)\sin(n\theta)\end{bmatrix}\cos(\omega t)\,,\ i=t,\,c,\,b, \tag{11}$$

where n is the number of circular waves. Functions $U_i(\xi)$, $V_i(\xi)$, $W_i(\xi)$, $X_i(\xi)$, $Y_i(\xi)$ (11) satisfy the boundary conditions (10). They have the following form:

$$U_i(\xi)=\sum_{m=1}^{N_u}U_m^{(i)}\Psi_m^{(U)}(\xi)\,;\quad V_i(\xi)=\sum_{m=1}^{N_v}V_m^{(i)}\Psi_m^{(V)}(\xi)\,;\quad W_i(\xi)=\sum_{m=1}^{N_w}W_m^{(i)}\Psi_m^{(W)}(\xi)\,;$$

$$X_i(\xi)=\sum_{m=1}^{N_x}X_m^{(i)}\Psi_m^{(X)}(\xi)\,;\quad Y_i(\xi)=\sum_{m=1}^{N_y}Y_m^{(i)}\Psi_m^{(Y)}(\xi)\,, \tag{12}$$

where $\Psi_m^{(U)}(\xi)$, $\Psi_m^{(V)}(\xi)$, $\Psi_m^{(W)}(\xi)$, $\Psi_m^{(X)}(\xi)$, $\Psi_m^{(Y)}(\xi)$ are basic functions; $U_m^{(i)}$, $V_m^{(i)}$, $W_m^{(i)}$, $X_m^{(i)}$, $Y_m^{(i)}$ are unknown parameters to be calculated.

Potential energy of a sandwich shell U_Σ has the following form

$$U_\Sigma=U_t+U_c+U_b\,.$$

The kinetic energy of thin-walled structure can be given as

$$T_\Sigma=T_t+T_c+T_b\,.$$

To study linear vibrations, we will use Hamilton's principle

$$\int_0^{2\pi/\omega}(U_\Sigma-T_\Sigma)dt\to\min\,. \tag{13}$$

Equations (11, 12) are used in energies (7–9) and double integrals are calculated. As a result, we obtain

$$U_\Sigma=\widetilde{U}(A)\cos^2(\omega t)\,;\ T_\Sigma=\omega^2\widetilde{T}(A)\sin^2(\omega t)\,, \tag{14}$$

where $A=\left(U_1^{(t)},...,U_{N_u}^{(t)},U_1^{(c)},...,Y_{N_Y}^{(b)}\right)$ is the vector of unknowns. The dimension of this vector is $N_*=3(N_u+N_v+N_w+N_X+N_Y)$. Functions $\widetilde{U}(A)$, $\widetilde{T}(A)$ are a quadratic form with respect to the elements of the vector A. Equations (14) are used in (13). Taking this into account, we obtain

$$\widetilde{U}(A)-\omega^2\widetilde{T}(A)\to\min\,. \tag{15}$$

Condition (15) is transformed into a system of N_* algebraic equations

$$\frac{\partial}{\partial A_j}\left[\widetilde{U}(A)-\omega^2\widetilde{T}(A)\right]=0\,;\, j=1,\,\ldots,\,N_*. \tag{16}$$

Equations (16)are transformed into an eigenvalue problem, from which the eigenfrequencies and vibration modes are found.

Results of numerical simulations

The shell is clamped at both edges

In this section, we consider a shell clamped at both edges. The boundary conditions have the form (10). Then the basis functions of the expansions (12) are as follows:

$$\Psi_m^{(U)}(\xi)=\Psi_m^{(V)}(\xi)=\Psi_m^{(W)}(\xi)=\Psi_m^{(X)}(\xi)=\Psi_m^{(Y)}(\xi)=\sin\left[\frac{m\pi\xi}{L}\right].$$

The honeycomb structure is manufactured using FDM additive manufacturing technology from ULTEM 9085 material. The mechanical characteristics of this material were determined experimentally. The honeycomb structure (Fig. 1, b) is replaced by a homogenized orthotropic continuous medium. The finite element method is used to calculate the mechanical properties [11].

The geometric parameters of the honeycomb structure cells are as:

l_1=6.1054 mm; l_2=3.0527 mm; θ=60°; l_c=10 mm; $\overline{h}_c$=0.4 mm,

where $\overline{h}_c$ is the cell wall thickness; l_c is the height of the honeycomb structure. The honeycomb structure satisfies Hooke's law (1). Engineering steels of homogenized orthotropic continuous medium have the following numerical values:

$$E_{11}=2.91\text{ MPa};\ E_{22}=2.91\text{ MPa};\ E_{33}=215.1\text{ MPa};$$
$$\nu_{12}=0.972;\ \nu_{23}=0.0051;\ \nu_{13}=0.0042;\ \rho_c=253.189\text{ kg/m}^3; \tag{17}$$
$$G_{12}=1.118\text{ MPa};\ G_{23}=39.1\text{ MPa};\ G_{13}=39.1\text{ MPa}.$$

The upper and lower face layers are made of carbon fiber. Their elastic properties satisfy Hooke's law. Engineering steels of this material are as follows:

$$E_x=160\times10^9\text{ Pa};\ E_y=6.8\times10^9\text{ Pa};\ \nu_{xy}=0{,}32;\ \nu_{yx}=0.0136;$$
$$G_{xy}=800\times10^9\text{ Pa};\ G_{xz}=G_{yz}=4\times10^9\text{ Pa};\ \rho_t=\rho_b=1400\text{ kg/m}^3. \tag{18}$$

The geometric parameters of the structures have the following values: $\varphi=\pi/12$; $s_c^{(1)}$=2.354 m; $s_t^{(1)}$=2.33 m; $s_b^{(1)}$=2.313 m; $h_t=h_b=10^{-3}$ m; $h_c=10^{-2}$ m.

The results of the calculations of the first ten natural frequencies of structures vibrations are given in Table 1. The number of circular waves n is given in the first column of the table, the size of the eigenvalue problem is given in the second column of the table. The natural frequencies obtained by the Rayleigh-Ritz method are given in the third column. The natural frequencies calculated by the finite element method in ANSYS are given in the fourth column. The relative difference of the natural frequencies δ obtained by different methods is given in the fifth column. To analyze the convergence of the natural frequencies of vibrations of the structure, the eigenvalue problem was calculated with different dimensions. As follows from the calculations, the natural

Table 1. Natural frequencies of a clamped shell

n	N_*	ω, Hz	ω_{FEM}, Hz	δ
1	180	412.84	–	–
	210	412.25	–	–
	270	411.83	421.98	0.0240
2	180	431.29	–	–
	210	430.61	–	–
	240	430.1	438.45	0.019
3	180	449.92	–	–
	210	449.14	–	–
	240	448.56	455.76	0.0150
8	210	451.6	–	–
	240	450.80	–	–
	270	450.22	460.61	0.0220
77	210	452.73	–	–
	240	451.96	–	–
	270	451.41	462.27	0.0230
6	210	458.77	–	–
	240	458.06	–	–
	270	457.54	467.82	0.0220
9	210	459.88	–	–
	240	459.05	–	–
	270	458.46	466.99	0.0180
4	180	461.70	–	–
	210	460.85	–	–
	240	460.24	467.50	0.0150
5	180	464.27	–	–
	210	463.35	–	–
	240	462.71	471.14	0.0180
10	210	479.25	–	–
	240	478.42	482.81	0.0091

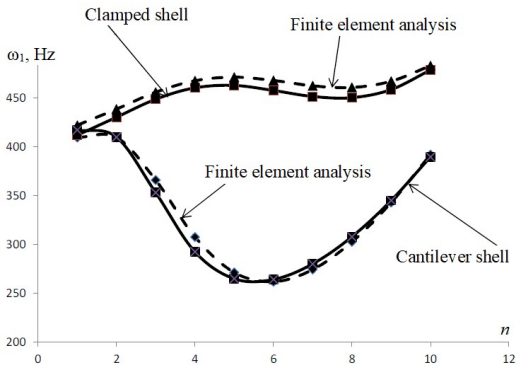

Fig. 2. Dependence of the first frequency ω_1 on the number of waves n

frequencies obtained by different methods are close. The spectrum of the natural frequencies is very dense. The first ten natural frequencies are observed in the range $\omega \in [411.83; 478.42]$ Hz. The dependence of the first natural frequency on the number of circular waves is shown by the solid curve in Fig. 2. The results of the finite element analysis are shown by the dashed line in Fig. 2. The minimum natural frequency of vibrations is observed at n=1. The minimum natural frequency of isotropic conical shells is observed at much higher values of n [12].

Cantilever shell

The results of numerical simulation of a cantilever conical shell are given in this paragraph. The shell edge with a larger radius is clamped, and the edge with a smaller radius is free. To satisfy the boundary conditions, the basis functions of the expansions (12) have the following form:

$$\Psi_m^{(U)}(\xi) = \Psi_m^{(V)}(\xi) = \Psi_m^{(W)}(\xi) = \Psi_m^{(X)}(\xi) = \Psi_m^{(Y)}(\xi) = \sin\left[\frac{(2m-1)\pi(L-\xi)}{2L}\right].$$

The mechanical characteristics of the upper and lower layers have the values (18), and the mechanical characteristics of the honeycomb structure have the form (17).

The natural frequencies of the cantilever shell are given in Table 2, and its columns have the same physical meaning as in Table 1. As follows from Table 2, the natural frequencies obtained by the Rayleigh-Ritz method and the finite element method coincide. The dependence of the first natural frequency on n is shown by a solid line in Fig. 2. The results of finite element modeling are given by a dashed line. The minimum vibration frequency is observed at n=6. The minimum frequency of the conical shell clamped on both sides is observed at n=1.

The linear vibrations of the cantilever sandwich shell are qualitatively different from the conical sandwich shell clamped on both ends, which follows from the results of the calculations given in Fig. 2.

Table 2. Natural frequencies of vibrations of the cantilever shell

n	N_*	ω, Hz	ω_{FEM}, Hz	δ
1	210	409.46	417.15	0.018
2	210	409.58	409.90	7.8×10^{-4}
3	210	365.95	353.16	0.036
4	210	307.81	292.54	0.050
5	210	271.49	265.06	0.020
6	210	262.10	264.29	0.006
7	210	274.41	280.20	0.020
8	210	302.77	307.97	0.016
9	210	342.96	345.00	0.006
10	210	391.95	389.58	0.006

Conclusions

The natural vibrations of a sandwich conical shell with a honeycomb structure manufactured by additive manufacturing technology FDM and various boundary conditions are considered. The stressed state of each layer is described by three displacements of the median surface of this layer and two angles of rotation of the normal to the median surface of the layer. The high-order shear theory is used to model the stressed state, and the Rayleigh-Ritz method is used to obtain the eigenvalue problem describing the natural vibrations of the structure. The vibrations of a three-layer sandwich shell are expanded into basis functions that satisfy the kinematic boundary conditions.

The element part of the mass matrix is close to zero due to the small thickness of the face layers and the small weight of the honeycomb structure, which allows reducing the dimensionality of the eigenvalue problem from which the vibration frequencies are calculated.

Linear vibrations of a truncated sandwich conical shell clamped on both sides and a cantilever shell are studied numerically. The minimum natural frequency of a sandwich conical shell clamped on both ends is observed when the number of waves in the circular direction is equal to one. The minimum natural frequency of a cantilever sandwich conical shell is observed when the number of waves in the circular direction is equal to six.

The results of semi-analytical calculations coincide with the results of finite element modeling in the ANSYS environment.

Financing

The above results were obtained under the project 2023.04/0001, funded by the National Research Foundation of Ukraine.

References

1. Karimiasl, M. & Ebrahimi, F. (2019). Large amplitude vibration of viscoelastically damped multiscale composite doubly curved sandwich shell with flexible core and MR layers. *Thin-Walled Structures*, vol. 144, article 106128. https://doi.org/10.1016/j.tws.2019.04.020.
2. Karimiasl, M., Ebrahimi, F., & Mahesh, V. (2019). Nonlinear forced vibration of smart multiscale sandwich composite doubly curved porous shell. *Thin-Walled Structures*, vol. 143, article 106152. https://doi.org/10.1016/j.tws.2019.04.044.
3. Cong, P. H., Khanh, N. D., Khoa, N. D., & Duc, N. D. (2018). New approach to investigate nonlinear dynamic response of sandwich auxetic double curves shallow shells using TSDT. *Composite Structures*, vol. 185, pp. 455–465. https://doi.org/10.1016/j.compstruct.2017.11.047.
4. Yadav, A., Amabili, M., Panda, S. K., Dey, T., & Kumar, R. (2021). Forced nonlinear vibrations of circular cylindrical sandwich shells with cellular core using higher-order shear and thickness deformation theory. *Journal of Sound and Vibration*, vol. 510, article 116283. https://doi.org/10.1016/j.jsv.2021.116283.
5. Van Quyen, N., Van Thanh, N., Quan, T. Q., & Duc, N. D. (2021). Nonlinear forced vibration of sandwich cylindrical panel with negative Poisson's ratio auxetic honeycombs core and CNTRC face sheets. *Thin-Walled Structures*, vol. 162, article 107571. https://doi.org/10.1016/j.tws.2021.107571.
6. Zhang, Y. & Li, Y. (2019). Nonlinear dynamic analysis of a double curvature honeycomb sandwich shell with simply supported boundaries by the homotopy analysis method. *Composite Structures*, vol. 221, article 110884. https://doi.org/10.1016/j.compstruct.2019.04.056.
7. Neigapula, V. S. N. & Sinha, P. K. (2007). Nonlinear free vibration analysis of laminated composite shells in hygrothermal environments. *Composite Structures*, vol. 77, pp. 475–483. https://doi.org/10.1016/j.compstruct.2005.08.002.
8. Li, C., Shen, H.-S., Wang, H., & Yu, Z. (2020). Large amplitude vibration of sandwich plates with functionally graded auxetic 3D lattice core. *International Journal of Mechanical Sciences*, vol. 174, article 105472. https://doi.org/10.1016/j.ijmecsci.2020.105472.
9. Li, Y., Li, F., & He, Y. (2011). Geometrically nonlinear forced vibrations of the symmetric rectangular honeycomb sandwich panels with completed clamped supported boundaries. *Composite Structures*, vol. 93, iss. 2, pp. 360–368. https://doi.org/10.1016/j.compstruct.2010.09.006.
10. Reinaldo Goncalves, B., Jelovica, J., & Romanoff, J. (2016). A homogenization method for geometric nonlinear analysis of sandwich structures with initial imperfections. *International Journal of Solids and Structures*, vol. 87, pp. 194–205. https://doi.org/10.1016/j.ijsolstr.2016.02.009.
11. Catapano, A. & Montemurro, M. (2014). A multi-scale approach for the optimum design of sandwich plates with honeycomb core. Part I: Homogenisation of core properties. *Composite Structures*, vol. 118, pp. 664–676. https://doi.org/10.1016/j.compstruct.2014.07.057.
12. Amabili, M. (2018). Nonlinear mechanics of shells and plates in composite, soft and biological Materials. Cambridge: Cambridge University Press. https://doi.org/10.1017/9781316422892.

Received 11 December 2024
Accepted 15 January 2025

Аналіз лінійних коливань композитної сандвіч-конічної оболонки, виготовленої адитивними технологіями

[1] К. В. Аврамов, [1] Б. В. Успенський, [2] Б. Г. Любарський, [2] О. А. Смецьких

[1] Інститут енергетичних машин і систем ім. А. М. Підгорного НАН України,
61046, Україна, м. Харків, вул. Комунальників, 2/10

[2] Національний технічний університет «Харківський політехнічний інститут»,
61002, Україна, м. Харків, вул. Кирпичова, 2

Сандвіч-конічна оболонка з пружним стільниковим заповнювачем, що досліджується в цій роботі, виготовляється адитивними технологіями та має три шари. Стільниковий заповнювач виробляється із матеріалу ULTEM, а горішні й долішні лицеві шари конструкцій – із вуглепластику. Кожен шар конструкцій є ортотропним матеріалом і задовольняє закону Гука. Завдяки процедурі гомогенізації, яка використовує метод скінчених елементів, замість стільникового заповнювача отримаємо еквівалентне ортотропне середовище. Пружні властивос-

ті цього середовища задовольняють закону Гука. Модифікована теорія зсуву високого порядку застосовується для моделювання деформування конструкцій. Деформування кожного шару конструкцій описуються п'ятьма змінними, до яких відносять три проєкції переміщень серединної поверхні і два кута повороту нормалі до серединної поверхні. Для розрахунку переміщень шарів використовуються граничні умови для напружень і граничні умови, які описують неперервність переміщень на межах шарів. Коливання тришарової сандвіч-оболонки розкладаються по базисних функціях, які задовольняють кінематичним граничним умовам. Для дослідження коливань використовується метод Релєя-Рітца. Параметри коливань конструкцій розраховуються із проблеми власних значень. Для верифікацій отриманих результатів власні частоти порівнюються з даними скінчено елементного моделювання. Як випливає із розрахунків, власні частоти, отримані методом Релєя-Рітца й методом скінченних елементів, близькі. Спектр власних частот дуже щільний. Мінімальна власна частота коливань спостерігається при числі хвиль у коловому напрямку рівнім одиниці.

***Ключові слова**: сандвіч-конічна оболонка, стільниковий заповнювач, лінійні коливання.*

Література

1. Karimiasl M., Ebrahimi F. Large amplitude vibration of viscoelastically damped multiscale composite doubly curved sandwich shell with flexible core and MR layers. *Thin-Walled Structures*. 2019. Vol. 144. Article 106128. https://doi.org/10.1016/j.tws.2019.04.020.
2. Karimiasl M., Ebrahimi F., Mahesh V. Nonlinear forced vibration of smart multiscale sandwich composite doubly curved porous shell. *Thin-Walled Structures*. 2019. Vol. 143. Article 106152. https://doi.org/10.1016/j.tws.2019.04.044.
3. Cong P. H., Khanh N. D., Khoa N. D., Duc N. D. New approach to investigate nonlinear dynamic response of sandwich auxetic double curves shallow shells using TSDT. *Composite Structures*. 2018. Vol. 185. P. 455–465. https://doi.org/10.1016/j.compstruct.2017.11.047.
4. Yadav A., Amabili M., Panda S. K., Dey T., Kumar R. Forced nonlinear vibrations of circular cylindrical sandwich shells with cellular core using higher-order shear and thickness deformation theory. *Journal of Sound and Vibration*. 2021. Vol. 510. Article 116283. https://doi.org/10.1016/j.jsv.2021.116283.
5. Van Quyen N., Van Thanh N., Quan T. Q., Duc N. D. Nonlinear forced vibration of sandwich cylindrical panel with negative Poisson's ratio auxetic honeycombs core and CNTRC face sheets. *Thin-Walled Structures*. 2021. Vol. 162. Article 107571. https://doi.org/10.1016/j.tws.2021.107571.
6. Zhang Y., Li Y. Nonlinear dynamic analysis of a double curvature honeycomb sandwich shell with simply supported boundaries by the homotopy analysis method. *Composite Structures*. 2019. Vol. 221. Article 110884. https://doi.org/10.1016/j.compstruct.2019.04.056.
7. Neigapula V. S. N., Sinha P. K. Nonlinear free vibration analysis of laminated composite shells in hygrothermal environments. *Composite Structures*. 2007. Vol. 77. P. 475–483. https://doi.org/10.1016/j.compstruct.2005.08.002.
8. Li C., Shen H.-S., Wang H., Yu Z. Large amplitude vibration of sandwich plates with functionally graded auxetic 3D lattice core. *International Journal of Mechanical Sciences*. 2020. Vol. 174. Article 105472. https://doi.org/10.1016/j.ijmecsci.2020.105472.
9. Li Y., Li F., He Y. Geometrically nonlinear forced vibrations of the symmetric rectangular honeycomb sandwich panels with completed clamped supported boundaries. *Composite Structures*. 2011. Vol. 93. Iss. 2. P. 360–368. https://doi.org/10.1016/j.compstruct.2010.09.006.
10. Reinaldo Goncalves B., Jelovica J., Romanoff J. A homogenization method for geometric nonlinear analysis of sandwich structures with initial imperfections. *International Journal of Solids and Structures*. 2016. Vol. 87. P. 194–205. https://doi.org/10.1016/j.ijsolstr.2016.02.009.
11. Catapano A., Montemurro M. A multi-scale approach for the optimum design of sandwich plates with honeycomb core. Part I: Homogenisation of core properties. *Composite Structures*. 2014. Vol. 118. P. 664–676. https://doi.org/10.1016/j.compstruct.2014.07.057.
12. Amabili M. Nonlinear mechanics of shells and plates in composite, soft and biological materials. Cambridge: Cambridge University Press, 2018. https://doi.org/10.1017/9781316422892.